COMBINING SANS WITH VSANS TO EXTEND Q-RANGE FOR MORPHOLOGY INVESTIGATION OF SILICON-GRAPHITE ANODES

Neelima Paul[a*], Henrich Frielinghaus[b], Sebastian Busch[c], Vitaliy Pipich[b], Ralph Gilles[a]

[a] *Heinz Maier-Leibnitz Zentrum, Technische Universität München, 85748 Garching, Germany*

* *e-mail:* Neelima.Paul@frm2.tum.de

[b]*Jülich Centre for Neutron Science (JCNS) at Heinz Maier-Leibnitz Zentrum (MLZ), Forschungszentrum Jülich GmbH, Lichtenbergstr. 1, 85748 Garching, Germany*

[c] *German Engineering Materials Science Centre (GEMS) at Heinz Maier-Leibnitz Zentrum (MLZ), Helmholtz-Zentrum Geesthacht GmbH, 85748 Garching, Germany*

Received July 2019

Abstract – Silicon-based electrodes are attractive candidates as anodes for Li-ion batteries due to their high theoretical specific capacity. However, repeated lithiation/delithiation causes significant morphological changes of the silicon particles which results in formation of highly porous silicon structures and severe side reactions at the silicon/electrolyte interface. To quantify such morphological changes in the micrometer as well as on the nanometer scale, we combine very small-angle neutron scattering (VSANS) and small-angle neutron scattering (SANS) techniques. While conventional and contrast-matched SANS data provide insights into the solid-electrolyte-interphase (SEI) coverage around the silicon particles and filling of the evolving porosity within the electrode, VSANS data provide information on the micrometer-sized graphite particles.

Keywords: Li-ion batteries, VSANS, SANS, Si-based anodes, SEI, pores, contrast variation

INTRODUCTION

Li-ion based rechargeable batteries with high specific energy are crucial for a wide variety of applications in consumer electronics and electromobility [1-2], and silicon-based

materials are attractive as anodes in batteries because of the nearly one order of magnitude higher theoretical capacity of silicon (3580 mAhg $^{-1}$ for $Li_{15}Si_4$) compared to the conventionally used graphite anode (372 mAhg $^{-1}$ for LiC_6) [3]. However, a major drawback of these electrodes is the expansion and contraction of silicon during alloying and dealloying with Li, respectively. This not only results in capacity fading, but also in transformation of initially compact silicon particles into expanded porous silicon particles. The initial charge/discharge cycles result in the formation of a solid-electrolyte-interphase (SEI) on the silicon-electrolyte interfaces. Wetjen et al. performed a detailed study on the electrochemistry and morphology of silicon-graphite (SiG) composite anodes and showed with help of STEM-EDS analysis that fluorine- and oxygen-containing SEI products cover the fragmented Si nanostructures [4]. With the STEM-EDS technique, it could not be verified if these elements were just coating the particle edges or also filling the pores. Using protonated and deuterated electrolytes, Paul et al. evaluated the mean pore size and pore size distribution in such porous Si nanoparticles and demonstrated the complete filling of pores with SEI products using contrast variation SANS [5]. This was the first time that SANS had been used to investigate SiG composite anodes. Earlier SANS studies in the field of Li-ion batteries had been based on graphite materials [6-8].

In the present work, we report results on SiG electrodes cycled with a standard FEC-containing electrolyte, which were additionally investigated using very small-angle scattering (VSANS), to gain insights on sample morphology in the micrometer scale, which can only be obtained by extending the Q-scale with VSANS.

EXPERIMENTAL DETAILS

Fresh SiG electrodes were prepared according to Ref [4]. To prepare the aged SiG electrodes, coin cells were constructed using a SiG anode, a LFP cathode, and two glass-fiber separators. Two different sets of electrolyte solutions were used for aging: (i) a standard FEC-containing electrolyte (1 M $LiPF_6$ in EC/EMC 3/7 g/g with FEC) and (ii) a pure EC electrolyte (1.5 M $LiPF_6$ dissolved in EC). After several charge/discharge cycles, (60 cycles for the standard FEC-containing electrolyte and 20 cycles for the pure EC electrolyte), SiG electrodes were extracted from cells in their fully discharged state and stored in a protective pouch-bag casing for ex-situ SANS and VSANS measurements.

Fig. 1 shows a SEM cross-sectional image of a pristine SiG sample where several ~ 200 nm Si particles are seen embedded in a matrix of micrometer-sized graphite particles. Fig. 2 shows STEM images of individual Si particles in fresh and aged SiG electrodes. The Si particle

in the fresh electrode is compact whereas the Si particle in the aged electrode seems expanded with interconnected Si fragments and pores.

The SANS measurements were performed at the SANS-1 instrument [9] of the Heinz Maier-Leibnitz Zentrum. A lower Q-limit of 0.004 $Å^{-1}$ was used to restrict the maximum resolved size by SANS to less than 200 nm and detect exclusively the scattering from nanosized inhomogeneities within and around expanded Si nanoparticles, without interference from SANS signal of the ~ 200 nm Si particles within a matrix of micrometer-sized graphite particles. The VSANS measurements were performed at the mirror focusing instrument KWS-3 [10] of the Heinz Maier-Leibnitz Zentrum to obtain information on the micrometer-sized graphite particles within Q-range 0.0001 $Å^{-1}$ and 0.0025 $Å^{-1}$. All measurements (SiG electrodes and calibration samples) were performed under ambient conditions. Thicknesses of all samples were included in the data reduction steps for an absolute calibration. The 2D isotropic scattering signals were radially averaged, and the resulting 1D data were plotted as differential cross-section versus the scattering vector Q. The VSANS data were corrected for multiple scattering effects because the corrections were considerable [11]. 1D data from VSANS and SANS were then merged to create a combined and extended Q range SANS plot of the fresh and the aged electrodes.

RESULTS AND DISCUSSIONS

In the first part of this section, we compare data of the fresh and aged electrodes cycled in a standard electrolyte, with standard SANS and VSANS to obtain information on the electrode morphology on the nanometer and micrometer length scale. In the second part, we will compare only the morphology on the nanometer length scale of the electrodes cycled in a pure EC electrolyte with contrast-matched SANS to obtain information on pore-filling.

Fig. 3 shows the combined VSANS and SANS data of the fresh and aged SiG electrodes, which were cycled in standard electrolyte. In the VSANS range, where micrometer-sized inhomogeneities in a matrix can be detected, scattering contributions from graphite flakes within the Si nanoparticles matrix are observed, which remain similar in both fresh and aged samples. Interestingly, in the SANS range, which is sensitive to nanometer-sized inhomogeneities in a matrix, the aged electrode shows a significantly higher scattering intensity compared to the fresh electrode. The increased scattering must be arising from nanometer sized lateral inhomogeneities of the expanded Si network, which were not present in the fresh SiG

electrode. Thus, they could be due to Si fragments, pores as well as due to SEI products surrounding the fragmented Si nanoparticles as all these did not exist in the fresh electrode. Due to the complexity of the 1D SANS curves no standard data treatment could be performed. The scattering from complex systems that contain multiple levels of related structural features such as the fractal structure of the Si particles over a wide Q-range need a different approach. The largest objects are the disc-like or platelet-like graphite particles whose diameter is too large to be observed in the scattering experiment. Therefore, the platelet thickness in the normal direction is considered as the first scattering term. It arises from a one-dimensional Fourier transform of a length ranging from −d to +d. From the SEM image in Fig. 1, one can see that the thickness is very well defined and gives rise to at least one minimum of the form factor. Other smaller structures appear much more polydisperse (i.e. length scales are distributed over a wider range), and so no oscillations are visible in the small-angle scattering.

The Beaucage model [12] applied on a double logarithmic scale allows to define linear ranges which can be fitted by power laws of the type $I(Q) \sim Q^{-P}$, each carrying the amplitudes A_i (i=2..4) together with the corresponding Guinier ranges. The parameters P_i define the fractal dimension and leads to information of surface or volume fractal structure on nanosized objects. The formula for our purpose looks like the following:

$$I(Q) = \left\{\left[A_1\left(\frac{\sin(Qd)}{Qd}\right)^2 + A_2\right]\exp\left(-\frac{Q^2R_2^2}{3}\right) + \frac{A_2P_2}{\Gamma(P_2)}\left(\frac{\mathrm{erf}^3\,(1.06QR_2/\sqrt{6})}{QR_2}\right)^{P_2} + A_3\right\}\exp\left(-\frac{Q^2R_3^2}{3}\right) + \frac{A_3P_3}{\Gamma(P_3)}\left(\frac{\mathrm{erf}^3\,(1.06QR_3/\sqrt{6})}{QR_3}\right)^{P_3} + A_4\exp\left(-\frac{Q^2R_4^2}{3}\right) + \frac{A_4\cdot 4}{\Gamma(4)}\left(\frac{\mathrm{erf}^3\,(1.06QR_4/\sqrt{6})}{QR_4}\right)^4 + \mathrm{bckgr}$$

with 2d (graphite particle thickness), A_i (forward scattering of fractal i), R_i (graphite particle thickness (i=2), Si interparticle distance (i=3) and radii of pores (i=4)), P_i (fractal dimension i), Γ (Gamma function), erf (error function) and bckgr (background). Specifically, SANS data have been modeled with the form factor of a platelet in the normal direction (term 1, which is a one-dimensional Fourier transform of a length from –d to +d) [13-14] and three stages of the Beaucage model [12] (terms 2-4) with arbitrary dimensionality P_i. For the first three terms the transition was influenced by the Guinier term of the succeeding term, while term 4 was added as a superposition (only for the aged electrode). So, the fresh electrode determined the overall modeling with terms 1-3, and term 4 was introduced to describe the difference to the aged electrode while only the amplitudes of the terms 1-3 were slightly varied. Terms 1 and 2 describe the same structure of a platelet particle (P_2 indicates the 2 dimensions) with $2d \approx 2R_2$

≈ 1 µm. This is in good agreement with the graphite platelet dimensions as confirmed with SEM image of Fig. 1. The next term describes a fractal at the borderline between a mass and surface fractal ($P_3 \approx 3$) with a typical size of 44 nm. This structure could arise from the spaces between the Si particles and resemble a house of cards as the representative for that fractal dimension. For the aged sample this contribution is doubled due to the swelling with electrolyte/SEI. The SEM image hardly resolves this structural size. The last term involves a single size of globules ($P_4 = 4$) with an average radius of 14.5 nm for the aged electrode that can be easily assigned to the pores within the expanded Si particles and confirmed by TEM images (Fig. 2). The final formula was programmed to the qtiKWS [15] software package in C++. Table I shows all parameters of the model fit. The entire morphological change in the SiG electrode before and after aging is shown in a very simplified schematic in Fig. 4.

To investigate if the porous Si network is filled with air or with SEI products, a contrast-matched study was performed where an EC electrolyte, whose scattering length density (SLD) is similar to that of the Si, was chosen for aging the electrode. This is because SEI products are formed from decomposed electrolyte and are expected to have a SLD similar to that of the electrolyte. Thus, SiG electrodes cycled in an EC electrolyte (SLD = 2.2×10^{-6} Å^{-2}) would only show SANS signal from pores if the pores are filled with air (SLD of air ~ 0 Å^{-2}) or are incompletely filled with SEI products. But if the pores are completely filled with SEI products, they would have SLD similar to that of the Si nanoparticle matrix (SLD=2.1×10^{-6} Å^{-2}) rendering them as well as SEI coatings 'invisible' to the surrounding Si nanoparticle matrix. In Fig. 5, a SANS plot of SiG electrode cycled in an EC electrolyte is shown along with the SANS plot of the fresh electrode. The SANS curves of the aged electrode shows almost no change on aging, which means the pores are completely filled with SEI products having the same SLD as the Si nanoparticle matrix. This indicates as well that pores are completely filled with SEI products and are only visible by SANS when the SLDs of their contents are strikingly different than that of the Si nanoparticle matrix.

In our previous study with similar SiG composites, we has shown using contrast matched SANS that the nanopores within the expanded Si nanoparticles are not empty but rather completely filled with SEI products [5]. However, using only the SANS technique, it had not been possible to investigate the impact of silicon morphology changes on graphite particle morphology, because the graphite particle sizes were in the micrometer scale. In the present study, we obtained both nanometer scale and micrometer scale morphological information of the same sample by combining their SANS and VSANS data. We concluded that there is no

negative impact of silicon morphology change on graphite particle morphology as the aged graphite particle size remains similar to the pristine graphite particle size.

SUMMARY

Combining the SANS and VSANS data on SiG battery electrodes, the resulting extended Q-range allowed to study both micrometer-sized as well as nanometer-sized structures (such as pores or particles) in these electrodes. Using an appropriate Beaucage model, quantitative and statistically averaged morphological information on graphite platelets, Si nanoparticles and nanopores over a large electrode volume was obtained. Furthermore, by planning an experiment where such electrodes are cycled in a specifically selected electrolyte, whose SLD is contrast-matched with that of Si, it was demonstrated that all pores in these expanded Si nanoparticles were accessible to electrolyte and were completed clogged with SEI products on electrode aging.

ACKNOWLEDGMENTS

This work was financially supported by the German Federal Ministry of Education and Research (BMBF) under the grant number 03XP0081 (ExZellTUM II). This work is based upon experiments performed at the SANS-1 instrument operated by HZG and FRM II as well as the KWS-3 instrument operated by JCNS at the Heinz Maier-Leibnitz Zentrum (MLZ), Garching, Germany. The authors thank the Heinz Maier-Leibnitz Zentrum (MLZ) for granting beam time at FRM II. Wacker Chemie AG is kindly acknowledged for providing the silicon nanoparticles.

REFERENCES

1. M. Winter, B. Barnett, K. Xu, Chem. Rev. **118**, 11433 (2018). DOI:10.1021/acs.chemrev.8b00422

2. M. Li, J. Lu, Z. Chen, K. Amine, Adv.Mater. **30**, 1800561 (2018). DOI: 10.1002/adma.201800561

3. M. N. Obrovac and V. L. Chevrier, Chem Rev, **114**, 11444 (2014). DOI:10.1021/cr500207g

4. M. Wetjen, S. Solchenbach, D. Pritzl, J. Hou, V. Tileli and H. A. Gasteiger, J. Electrochem. Soc., **165**, A1503 (2018). DOI:10.1149/2.1261807jes

5. N. Paul, M. Wetjen, S. Busch, H. Gasteiger and R. Gilles, J. Electrochem. Soc., **166**, A1051 (2019). DOI: 10.1149/2.0781906jes

6. E. P. Gilbert, P. A. Reynolds and J. W. White, J. Chem. Soc., Faraday Trans., **94**, 1861 (1998). DOI: 10.1039/A801303I

7. G. Sandi, K. A. Carrado, R. E. Winans, C. S. Johnson and R. Csencsits, J. Electrochem. Soc., **146**, 3644 (1999). DOI: 10.1149/1.1392527.

8. C. A. Bridges, X.-G. Sun, J. Zhao, M. P. Paranthaman and S. Dai, J. Phys. Chem. C, **116**, 7701 (2012). DOI: 10.1021/jp3012393

9. Heinz Maier-Leibnitz Zentrum et al. SANS-1: Small angle neutron scattering. Journal of large-scale research facilities, **1**, A10 (2015). DOI: 10.17815/jlsrf-1-32.

10. Heinz Maier-Leibnitz Zentrum et al. KWS-3: Very small angle scattering diffractometer with focusing mirror. Journal of large-scale research facilities, **1**, A31 (2015). DOI: 10.17815/jlsrf-1-28

11. H. Frielinghaus, Nucl. Instrum. Meth. A, **904**, 9 (2018). DOI: 10.1016/j.nima.2018.07.027

12. G. Beaucage, J. Appl. Cryst. **28**, 717 (1995). DOI: 10.1107/S0021889895005292

13. J.S. Pedersen, J. Appl. Cryst. **33**, 637 (2000). DOI: 10.1107/S0021889899012248

14. J.S. Pedersen, Adv. Coll. Interf. Sci. **70**, 171 (1997) DOI: 10.1016/S0001-8686(97)00312-6)

15. http://iffwww.iff.kfa-juelich.de/~pipich/dokuwiki/doku.php/qtikws

FIGURES CAPTIONS

Fig. 1. An SEM cross-sectional image of the fresh SiG electrode shows ~ 200 nm compact spherical Si particles embedded within a graphite matrix of µm-sized flaky graphite particles. Adapted from Wetjen et al. [4] with permission from The Electrochemical Society (Copyright 2018).

Fig. 2. STEM images of individual Si particles in fresh (uncycled) and aged SiG electrodes show that the initially ~200 nm Si nanoparticle has expanded in size to about ~400 nm on aging. Adapted from Wetjen et al. [4] with permission from The Electrochemical Society (Copyright 2018).

Fig. 3. Radially averaged 1D SANS and VSANS data of fresh SiG (black circles) and aged SiG (red squares) electrode, covering together a Q range from 0.0001 $Å^{-1}$ to 0.7 $Å^{-1}$. In the SANS range, the aged SiG electrode shows a significantly higher scattering due to presence of nanopores within the Si nanoparticles, the SEI layer around them and the fragmented Si filaments. In the VSANS range, scattering contributions from graphite flakes interdispersed between the Si nanoparticles are observed, which remain similar in both fresh and aged samples with an average width of ~1 µm. The solid lines show the fit of the data with a Beaucage model. The term 1 describes form factor of the graphite platelet in normal direction, term 2 refers to the graphite platelet fractal tail, term 3 refers to the Si interparticle scattering, and the Term 4 refers to the scattering from pores.

Fig. 4. A very simplified cartoon of fresh and aged SiG electrodes. Si nanoparticles are embedded within a matrix of micrometer sized graphite particles. On aging, the initially compact Si nanoparticles expand and form porous structures containing nanosized pores, which get filled with SEI products. The graphite particles appear not to change in size.

Fig. 5. Radially averaged 1D SANS data of fresh SiG (black circles) and aged SiG (red squares) electrode. The SiG electrode was cycled in protonated EC electrolyte to match the scattering contrast of the SEI products with that of the Si nanoparticle. The SANS data of fresh and aged electrodes look similar, or in other words, nanostructures in the aged electrodes 'virtually disappear'. This confirms the complete filling or clogging of pores within Si nanoparticles with SEI products.

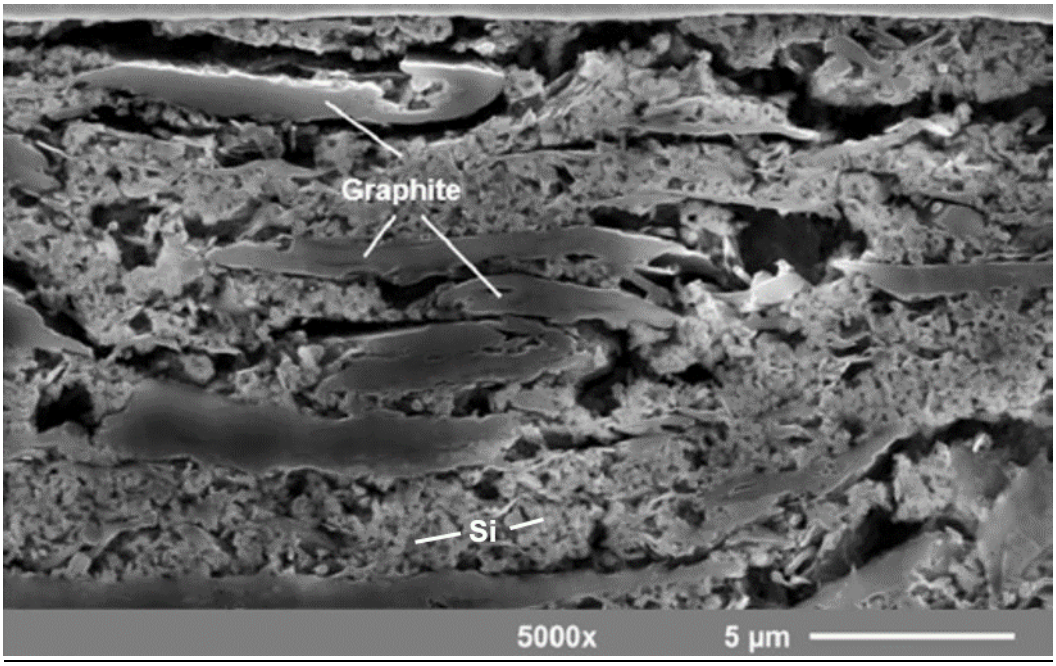

Fig. 1. N. Paul, *Journal of Surface Investigation*

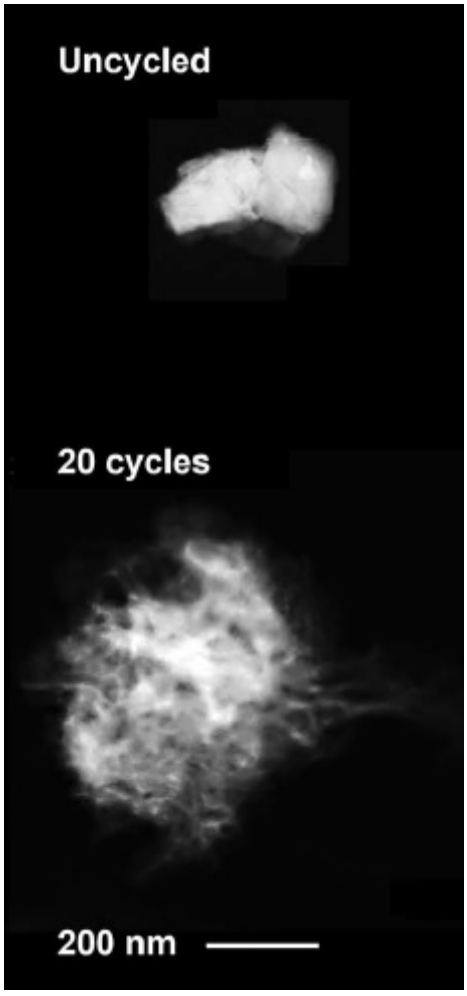

Fig. 2. N. Paul, *Journal of Surface Investigation*

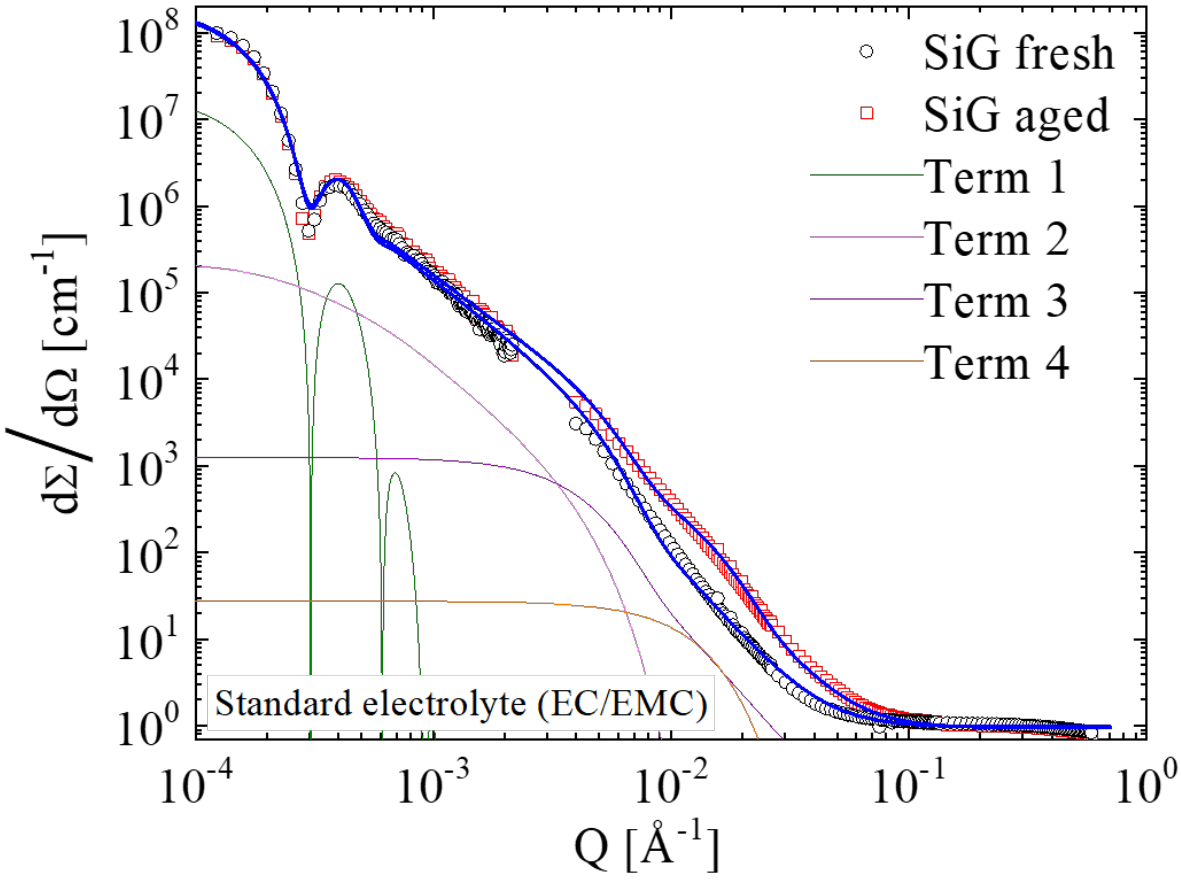

Fig. 3. N. Paul, *Journal of Surface Investigation*

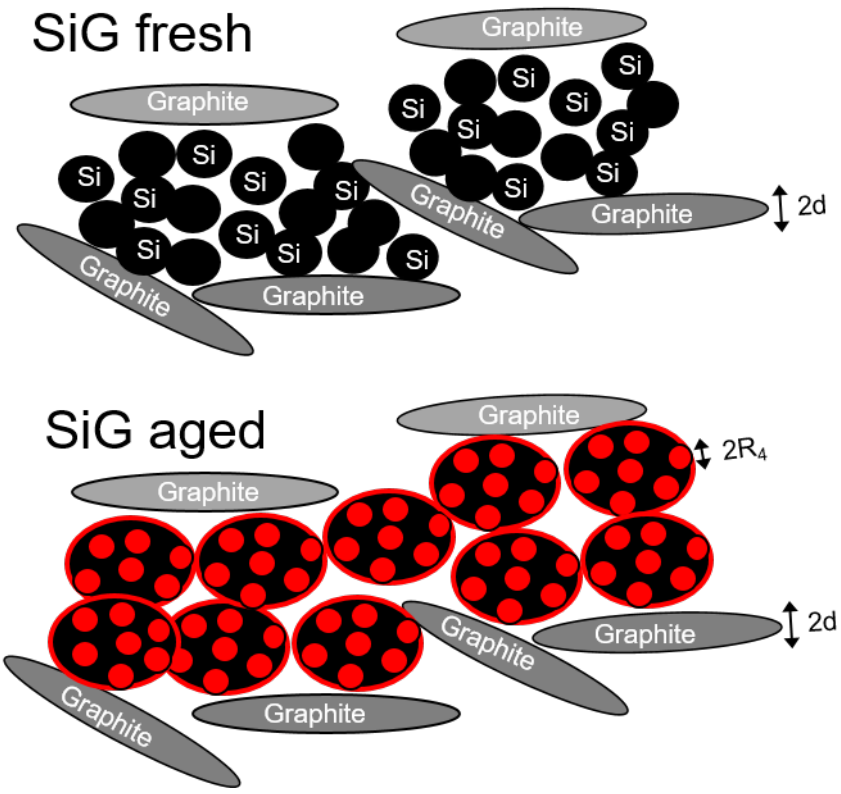

Fig. 4. N. Paul, *Journal of Surface Investigation*

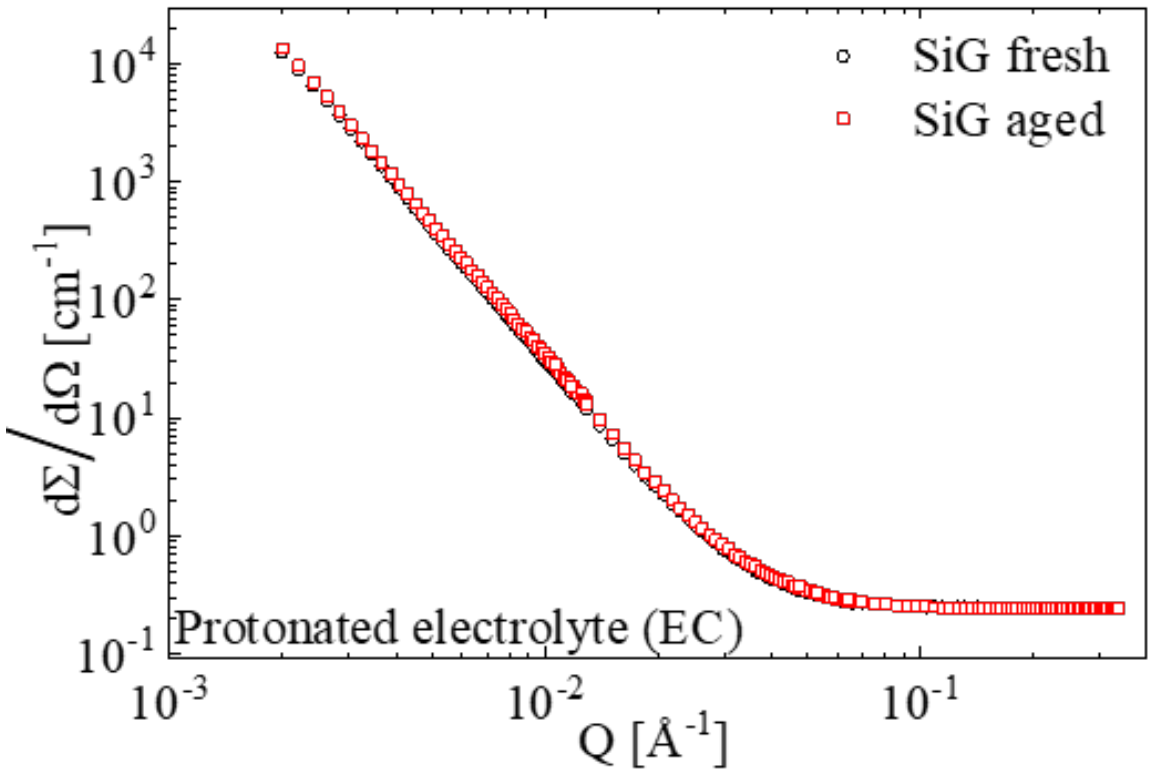

Fig. 5. N. Paul, *Journal of Surface Investigation*

Table I: Parameters corresponding to the fit to data according to Beaucage model.

Parameter	Fresh SiG electrode	Aged SiG electrode	Description of parameters
A_1 [cm^{-1}]	$(2.11\pm0.16)\times10^8$	$(2.03\pm0.10)\times10^8$	prefactor (number density of fractals)
2d [nm]	1030±8	fix 1030	graphite particle thickness
A_2 [cm^{-1}]	$(2.06\pm0.26)\times10^6$	$(2.27\pm0.04)\times10^6$	prefactor (number density of fractals)
R_2 [nm]	590±18	fix 590	radii graphite particle thickness from fractal scattering, i.e radius in 1D
P_2	2.10±0.02	fix 2.10	fractal dimension
A_3 [cm^{-1}]	5600±1900	12500±600	prefactor (number density of fractals)
R_3 [nm]	44±2.5	fix 44	Si interparticle distance
P_3	3.06±0.06	fix 3.06	fractal dimension
A_4 [cm^{-1}]	--	274±37	prefactor (number density)
R_4 [nm]	--	14±0.4	radii of pores
bckgr. [cm^{-1}]	0.974±0.017	0.946±0.018	background